

Analysis of Snow Cover in Alaska using Aircraft Microwave Data (April 1995)

D. K. Hall*
 J. L. Foster*
 A. T. C. Chang*
 D. J. Cavalieri**
 J. R. Wang***

*Hydrological Sciences Branch, Code 974

**Oceans and Ice Branch, Code 971

***Microwave Sensors Branch, Code 975

Laboratory for Hydrospheric Processes

NASA/Goddard Space Flight Center

Greenbelt, MD 20771

E-mail: dhall@glacier.gsfc.nasa.gov

and

C. S. Benson
 Geophysical Institute
 University of Alaska
 Fairbanks, AK 99775-7320

ABSTRACT

During April of 1995, a field and aircraft experiment was conducted in central and northern Alaska. A Millimeter-wave Imaging Radiometer (MIR), and other sensors, were flown on-board a NASA ER-2 aircraft in a grid pattern centered over Fairbanks. Resulting MIR data show brightness temperature patterns that are related to land cover and snowmelt patterns.

INTRODUCTION

From 31 March to 25 April, 1995, a mission was conducted to study snow cover in northern and central Alaska, respectively. The utility of high frequency passive-microwave aircraft data is assessed as is the influence of a variety of surface cover types on the microwave brightness temperatures of dry and melting snow. The aircraft data included the Millimeter-wave Imaging Radiometer (MIR) and the Moderate Resolution Imaging Spectroradiometer (MODIS) Airborne Simulator (MAS). Analysis of MAS data will be discussed in a subsequent paper. In this paper, the MIR data are analyzed along with ground-truth and meteorological data that were acquired simultaneous with the aircraft overpasses in the series of aircraft flights flown over Fairbanks.

AIRCRAFT INSTRUMENTATION

The MIR is a mechanically-scanned imaging microwave radiometer that measures radiation at the following frequencies: 89, 150, 183.3±1, 183.3±3, 183.3±7 and 220 GHz. It has an angular resolution of about 3.5°. It is a cross-track scanner with an angular swath width of about 100°, centered at nadir. Its polarization vector is in the horizontal plane and perpendicular to the velocity vector of the aircraft so that the measured radiation is a mixture of vertical and horizontal polarizations depending on the viewing angles. The temperature sensitivity is ≤ 1 K for all channels. The 183.3-GHz channels are not used in this work due to its location in the water vapor absorption line. The MIR data in this study have a spatial resolution of approximately 1 km at nadir.

BACKGROUND

The ability to infer snowpack thickness using passive-microwave data has been recognized for many years. However, many factors have been found that complicate the relationship between passive microwave brightness temperature and snow depth [1]. For example, snow grain size differences [2], [3] and forest cover [4], [5] influence the brightness temperature of snowpacks, and there is a strong

dependence of microwave brightness temperature on topography and land cover [2].

Chang et al. [6] found that 92-GHz aircraft data, acquired over Alaska during a 1983 experiment, was more sensitive to snow-crystal scattering than was 37-GHz data, but was also more sensitive to atmospheric parameters. In cloud-free areas, 37- and 92-GHz brightness-temperature patterns over snow in Alaska were similar. However, at 92 GHz, the atmospheric brightness temperature contribution is much higher than it is at 37 GHz, 50 K in the subarctic winter and 100 K in the subarctic summer [6].

METHODOLOGY

Field measurements of snow depth, density, grain size and shape were made in Fairbanks (64°50'N, 147°48'W) and at Ester Dome which is about 5 km northwest of Fairbanks, as well as in other parts of Alaska. Aircraft flight lines were flown in a grid pattern in central Alaska, including Fairbanks, on 5, 6, 13 and 21 April. These data have been gridded to a polar stereographic equal area map. In addition, a vegetation map of Alaska [7] was registered to the MIR data to compare with the aircraft data.

RESULTS AND DISCUSSION

Field and air-temperature measurements showed that the snow in and near Fairbanks was melting during the daytime during the month of April. Except within the city, snow cover was nearly continuous. Table 1 shows snow depths from a location in Fairbanks and at Ester Dome. Table 2 shows air temperatures at the approximate time of the aircraft takeoff on the flight days over the 'Fairbanks grid.' Each flight over the Fairbanks grid lasted about 2 hours and 20 minutes.

Table 1. Snow depths in Fairbanks and at Ester Dome on selected dates in April.

<u>Date</u>	<u>Fairbanks</u>	<u>Ester Dome</u>
4/1/95	59 cm	---
4/2/95	54 cm	---
4/6/95	39 cm	---
4/7/95	35 cm	---
4/8/95	---	100 cm
4/11/95	23 cm	---

Table 2. Average air temperatures at approximate times of aircraft takeoffs, and time of flights over the 'Fairbanks grid.'

<u>Date</u>	<u>°C</u>	<u>Fairbanks local time</u>
4/5/95	8°	10:50 - 13:11
4/6/95	3°	8:42 - 11:01
4/13/95	10°	11:08 - 13:36
4/21/95	-1°	6:59 - 9:29

Analysis of the MIR 89-, 150- and 220-GHz data shows that the brightness temperature increases with frequency, due to increased emission from the atmosphere as discussed by Chang et al. [6]. For example, on 5 April, the 89-, 150- and 220-GHz MIR brightness temperatures averaged 263, 264 K and 269 K, respectively, in the vicinity of Fairbanks.

Snow in Fairbanks was actively melting during the daytime during the month of April. As soon as snow becomes wet, scattering is reduced as the crystals become coated with liquid water. As a result, the snowpack behaves as a lossy medium, and the brightness temperature increases. In the vicinity of Fairbanks, the 89-GHz brightness temperatures averaged 263 K, while in the southern part of the study area (central Alaska Range) brightness temperatures were \approx 210 K on 5 April. Deeper snow and lower temperatures caused the brightness temperatures to be lower there. Additionally, on lines flown north of Fairbanks, toward the Brooks Range and on the North Slope, also on 5 April, brightness temperatures are 10-40 K lower than in the Fairbanks area because the snow to the north was still dry in April (Figure 1). Also, in the Brooks Range and on the North Slope, there are no trees to increase the brightness temperatures there.

Comparison of the vegetation map with the MIR data shows that several land-cover types influence the microwave signal. On each of the 4 MIR images (at 89 GHz) for the Fairbanks grid, the boundary between the black spruce forest and the meadow dryas is evident at a latitude of approximately 64°N, just south of Fairbanks (Figure 1). Coniferous trees emit more microwave radiation than do tundra or dryas vegetation, and this is one explanation for the higher brightness temperatures in the black spruce forests.

In the central part of the Fairbanks grid, brightness temperatures are generally quite high due to the melting snow. The relatively high brightness temperatures there overwhelm the brightness-temperature differences that result from land-cover variability. This is especially true on April 13, when the air temperatures were the highest of the 4 flight days (Table 2), and presumably, when melting covered the largest extent of area.

On 6 April, note in Figure 1 that brightness temperatures are quite low over the Fairbanks grid as compared to the other days. The air temperature as recorded at Fairbanks was 3°C, but may have actually been below freezing over most of the Fairbanks grid. If this were the case, and the snowpack was dry, this would explain the much-lower brightness temperatures measured during the 6 April flight, and the closer match between brightness temperatures there and to the north.

Other regions of interest are where finger-like projections of the spruce-birch forest to the east of Fairbanks intersect dryas meadows and barren areas. Brightness temperatures are higher in the spruce-birch forest (≈ 261 K) than in the dryas meadows and barren areas (≈ 251 K) presumably due to the higher emissivity of the trees.

CONCLUSIONS AND FUTURE WORK

The land-cover type is shown to influence microwave brightness temperature under dry snow conditions. Snow-covered forests cause higher brightness temperatures than do snow-covered dryas meadows and tundra. However, when the snowpack is wet, the high emissivity of the snowpack overwhelms the contribution of the vegetation to the brightness temperature.

Work will continue on the current data set to investigate the influence of land cover particularly the influence of the dryas meadows and black spruce. Satellite data will be analyzed in conjunction with MIR data in order to modify snow depth retrieval algorithms so that they are more responsive to the snow and land surface conditions encountered in central and northern Alaska.

ACKNOWLEDGMENTS

The authors would like to thank Janet Chien for her expertise in preparing the MIR data for analysis, Penny Masuoka for digitizing Kuchler's vegetation map, and NASA Ames Research Center for the aircraft support. Work was supported by NASA's Mission to Planet Earth project office.

REFERENCES

1. A.T. C. Chang, J.L. Foster, D.K. Hall, B.E. Goodison, A.E. Walker, J.R. Metcalfe and A. Harby, "Snow parameters derived from microwave measurements during the BOREAS winter field campaign, submitted to *Journal of Geophysical Research*, in press.
2. D.K. Hall, C.S. Benson and J.Y.L. Chien, "Analysis of visible and microwave satellite data for snow mapping in

Alaska," *Proceedings of the 50th Eastern Snow Conference*, Quebec City, pp. 129-137, 1993.

3. R. Armstrong, A.T.C. Chang, A. Rango and E.G. Josberger, "Snow depth and grain size relationships with relevance for passive microwave studies," *Annals of Glaciology*, vol. 17, pp.171-176, 1993.
4. M. Tiuri and M. Hallikainen, "Remote sensing of snow depth by passive microwave satellite observations," *Proceedings of the 11th European Microwave Conference*, Amsterdam, pp. 233-238, 1981.
5. D.K. Hall, J.L. Foster and A.T.C. Chang, "Measurement and modeling emission from forested snow fields in Michigan," *Nordic Hydrology*, vol. 13, pp. 129-138, 1982.
6. Chang, A.T.C., J.L. Foster and D.K. Hall, 1987: Microwave snow signatures (1.5 mm to 3 cm) over Alaska, *Cold Regions Science and Technology*, vol. 13, pp. 153-160.
7. Kuchler, A.W., 1985: Potential Natural Vegetation, USGS Map from *National Atlas*, sheet no. 89.

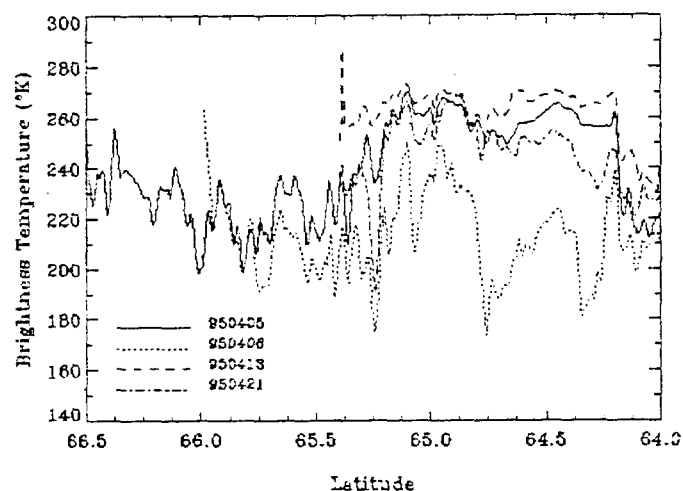


Figure 1. 89-GHz data from transects of MIR imagery showing brightness-temperature changes from northern Alaska to southern Alaska. Note that not all of the flights were flown of the same areas on each day.

Comparison of Aircraft and DMSP SSM/I Passive Microwave Measurements Over the Bering Sea in April 1995

D. J. Cavalieri, D. K. Hall, and J. R. Wang

Laboratory for Hydrospheric Processes

NASA Goddard Space Flight Center Greenbelt, Maryland 20771 U.S.A.

Tel: (301) 286-2444 Fax: (301) 286-0240 Email: don@cavalieri.gsfc.nasa.gov

Abstract - During April 1995 a NASA ER-2 high-altitude aircraft carrying a Millimeter-Wave Imaging Radiometer (MIR) made two flights over the Bering Sea as part of a mission to study sea ice and snow for improving retrievals of these parameters from passive microwave radiometers. MIR measures radiances at 89 GHz, 150 GHz, three frequencies near 183 GHz, and at 220 GHz. Sea ice features are observable at all frequencies except at 183 GHz, because of strong atmospheric water vapor absorption. The radiometric brightness over ice-free ocean increases with frequency as expected, but the situation is more complex over sea ice.

INTRODUCTION

A NASA ER-2 high-altitude aircraft made a series of flights over Alaska and the Bering Sea in April 1995 in support of sea ice and snow algorithm development for the NASA MTPE EOS AMSR and MODIS instrument science teams. The two primary sensors aboard the ER-2 were a six-channel, total power Millimeter-Wave Imaging Radiometer (MIR) and a Moderate Resolution Imaging Spectroradiometer Airborne Simulator. This paper reports on the results obtained with the MIR over the Bering Sea ice cover on April 8.

Sea ice retrievals from satellite passive microwave radiometers are sensitive to atmospheric water vapor variability. This is particularly the case in the vicinity of the ice edge and in marginal sea ice zones where ice concentrations are low. Some studies have examined the effect of water vapor variability on sea ice retrievals at lower frequencies (18 and 37 GHz) [1], but little work has been done at higher frequencies (85 GHz and higher). The MIR range of frequencies (89 GHz to 220 GHz) have been used previously for determining water vapor profiles over the ocean surface [2] and may, in combination with the lower frequency channels on the Defense Meteorological Satellite Program (DMSP) Special Sensor Microwave/Imager (SSM/I), also be useful in assessing and improving current methods of eliminating the effects of water vapor variability on sea ice retrievals [3]. This paper examines the spectral variation of MIR radiances over the Bering Sea ice cover and compares this variation to the known properties of the ice cover as determined from the DMSP SSM/I.

DATA

The DMSP SSM/I radiances are used with the NASA Team sea ice algorithms [4,5] to provide a description of the Bering Sea ice cover. On April 8 the ice cover extended to 55.6° N, 194° E in the southeastern portion of the Bering Sea and to 60° N, 180° E in the western portion. The sea ice concentration was generally high (85-100%), except in the marginal ice zone and in coastal polynyas. The largest coastal polynya was located south of St. Lawrence Island (SLI) where the minimum observed concentration at the mapped resolution of 25 km was 45%. From the NASA thin ice algorithm [5] only two areas along the aircraft flight path show the presence of new and young ice; one is a coastal polynya in the eastern most end of Norton Sound and the other is the SLI polynya.

The ER-2 MIR is a cross-track scanner that has a 3-dB beam width of 3.5° and an angular swath of 100°. At a nominal aircraft altitude of 18.5 km, the ground resolution at nadir is about 1 km. It measures a mixture of horizontal and vertical polarizations at 89 GHz, 150 GHz, 183±1 GHz, 183±3 GHz, 183±7 GHz, and at 220 GHz. The polarization mix varies with incidence angle, but this effect is small over sea ice. There is generally good agreement between the MIR 89 GHz observations and the averaged 85.5 GHz horizontally and vertically polarized DMSP SSM/I data. The ER-2 aircraft flight tracks over the Bering Sea were planned to optimize coverage of as many SSM/I footprints as possible while still imaging a range of sea ice types and ice-free ocean.

RESULTS

The April 8 MIR radiance maps for 89 GHz, 150 GHz, and 220 GHz are shown in Fig. 1, 2, and 3 respectively. These figures show sea ice areas which exhibit contrasting spectral variations along the flight path. The first is an area of consolidated sea ice off of Nome, Alaska. MIR brightness temperatures range from 190 K to 210 K at 89 GHz, from 175 K to 200 K at 150 GHz, and from 200 K to 210 GHz at 220 GHz. The lower radiances observed at 150 GHz are not consistent with the expected increase in brightness with frequency resulting from atmospheric water vapor emission. Examination of the 85 GHz SSM/I data at horizontal and vertical polarization also shows this area of relatively low brightness. This is not observed,



175

265

Figure 1: MIR 89 GHz image of the Bering Sea ice cover for April 8, 1995.

however, at lower frequencies or in the polarization, $(V-H)/(V+H)$, at 85 GHz. This decrease in brightness at 150 GHz relative to the other two MIR frequencies is also observed in the region just north of SLI.

In contrast to this spectral variation is the increase in brightness temperature with frequency observed in the polynya south of SLI (see Fig. 1, 2, and 3). Near the SLI coastline, the MIR brightness temperatures increase from about 200 K at 89 GHz, to 220 K at 150 GHz, and to 240 K at 220 GHz. The spatial pattern of radiances observed in the figures suggests the presence of clouds (or water vapor) emanating from over the polynya and spreading southward. This is not inconsistent with a characteristic feature of polynyas. An increase in brightness with MIR frequency is also observed further south in the marginal ice zone, a transition region of lower ice concentration,

and over ice-free ocean.

CONCLUSIONS

The contrasting spectral variations observed in MIR data at 89, 150, and 220 GHz over the Bering Sea ice cover on April 8 suggest that both atmospheric emission and surface influences are affecting the received radiances. In a region off of Nome, Alaska and just north of SLI, the lower brightness at 150 GHz relative to the other two frequencies suggests the occurrence of surface scattering. This scattering may result from a particularly heavy snow cover on the sea ice. This effect has been observed north of SLI in previous aircraft missions [6]. Over ice-free ocean or areas of low ice concentration, as for example, in the vicinity of coastal polynyas, the increase of brightness temperature with frequency is consistent with a spectral response one would expect from an atmosphere with appreciable water vapor. Further work is needed to determine quantitatively the contributions from surface scattering and atmospheric water vapor variability.

ACKNOWLEDGMENTS

The aircraft flights and data analysis were supported by the NASA MTPE EOS Project Office. We thank the High Altitude Missions Branch at NASA Ames Research Center for the successful ER-2 aircraft mission.

REFERENCES

- [1] Wang, J. R. and L. A. Chang, Retrieval of water vapor profiles from microwave radio-metric measurements near 90 Hz and 183 GHz, *Journal of Applied Meteorology*, 29, 1005-1013, 1990.
- [2] Cavalieri, D. J., K. St. Germain and C. Swift, Reduction of Weather Effects in the Calculation of Sea Ice Concentration with the DMSP SSM/I, *J. Glaciology*, 41, 455-464, 1995.
- [3] Maslanik, J. A., Effects of weather on the retrieval of sea ice concentration and ice type from passive microwave data, *Int. J. Remote Sensing*, 13, 37-54, 1992.
- [4] Cavalieri, D. J., J. Crawford, M. R. Drinkwater, D. Eppler, L. D. Farmer, R. R. Jentz and C. C. Wackerman, Aircraft active and passive microwave validation of sea ice concentration from the DMSP SSM/I, *J. Geophys. Res.*, 96, 21,989-22,008, 1991.
- [5] Cavalieri, D. J., A microwave technique for mapping thin sea ice, *J. Geophys. Res.*, 99, 12,561-12,572, 1994.
- [6] Cavalieri, D. J., P. Gloersen and T. T. Wilheit, Aircraft and satellite passive microwave observations of the Bering Sea ice cover during MIZEX-West, *IEEE Transactions on Geoscience and Remote Sensing*, GE-24, 368-377, 1986.



175 255

Figure 2: MIR 150 GHz image of the Bering Sea ice cover for April 8, 1995.



175 255

Figure 3: MIR 220 GHz image of the Bering Sea ice cover for April 8, 1995.

Recent Progress in Development of the Moderate Resolution Imaging Spectroradiometer Snow Cover Algorithm and Product

George Riggs

Research and Data Systems Corp., 7833 Walker Drive, Suite 550, Greenbelt, MD 20770, tel 301-286-6811, e-mail griggs@ltpmail.gsfc.nasa.gov

Dorothy K. Hall

Code 974, NASA/GSFC, Greenbelt, MD 20771, tel 301-286-6892, fax 301-286-1758, email dhall@glacier.gsfc.nasa.gov

Vincent V. Salomonson

Code 900, NASA/GSFC, Greenbelt, MD 20771, tel 301-286-8601, fax 301-286-1738, email vinces@farside.gsfc.nasa.gov

Abstract -- In preparation for the launch of the Moderate Resolution Imaging Spectroradiometer (MODIS) on the first NASA Earth Observing System platform in 1998, an algorithm to generate a global snow cover map is being developed. Status of the snow mapping algorithm and description of the data product is described in this paper.

INTRODUCTION

Monitoring the spatial and temporal extent of seasonal snow cover at synoptic, regional and local scales is important to the research, modelling and operational monitoring communities concerned with snow cover [1]. A snow algorithm and data product are being developed for the future Moderate Resolution Imaging Spectroradiometer (MODIS) instrument to be flown aboard the Earth Observing System (EOS), a part of NASA's Mission to Planet Earth (MTPE). Landsat Thematic Mapper (TM) and MODIS Airborne Simulator Data (MAS) are used as surrogates for MODIS data during development of the algorithm.

BACKGROUND

The objective for the MODIS snow algorithm, SNOMAP, is to generate a consistent, well described, global snow cover data product. The spatial resolution planned for the snow cover data product is 500 m with daily and ten day composites of the product generated and archived.

MODIS is an imaging radiometer consisting of a cross track scan mirror, collection optics and set of linear detector arrays with spectral interference filters in four focal planes. MODIS has 36 discrete bands between 0.4 and 15 μm selected for diagnostic significance in Earth science. The different spectral bands have spatial resolutions of 250 m, 500 m or 1 km at nadir. Complete description of the MODIS instrument can be found at the MODIS homepage <http://ltpwww.gsfc.nasa.gov/MODIS/MODIS.html>. Orbital characteristics of the EOS platform will allow MODIS to have near daily repeat coverage over much of the globe and in

the mid to upper latitudes swath overlap will provide multiple daily views of some regions. Those multiple views open the option of the algorithm to select and analyze the "best" observation(s) of a location for the day.

Processing and generation of MODIS data products will be done at several levels. The levels are defined by temporal and spatial manipulations done on the data to arrive at a product. Information about the data processing system and these data levels can be found at the Earth Observation System and Data Information System (EOSDIS) home page <http://spsosun.gsfc.nasa.gov/ESDIShome.html>. The lowest level is a short segment of an orbital swath, while the next levels involve spatial and temporal manipulations, including gridding of data, to generate products covering larger spatial areas. Within the MODIS land group of investigators there is a gridding and tiling scheme to assemble MODIS swaths into geographically referenced and gridded tiles for common use among products.

The SNOMAP algorithm is composed of three algorithms for product generation at the swath level, daily composite, and ten day composite. Products from the swath flow to daily compositing, which flow to the ten day composite. Ten day compositing follows the compositing scheme laid out by the Science Working Group [EOS] AM Platform (SWAMP). The ten day compositing periods are defined as: first ten days of the month, days 11 - 21, then day 21 to end of month.

Other MODIS data products such as the cloud mask and static land/water mask are being integrated into SNOMAP to mask large water bodies and assist with discriminating snow from cloud. For information on other MODIS data products and the Earth Science Data Information System (ESDIS) in general begin at <http://spsosun.gsfc.nasa.gov/ESDIShome.html>.

The snow cover products are generated in HDF format composed of global attributes (metadata), product specific attributes (metadata and quality information) and the snow cover 'map' as a scientific data array.

TECHNIQUE

The SNOMAP algorithm at the swath level employs criteria tests and decision rules with universal threshold values, to identify snow by its reflectance features in the visible and near infrared wavelengths (NIR). Techniques are briefly described here; greater discussion is presented in [2]. A principle key to identification of snow is the Normalized Difference Snow Index (NDSI). The NDSI is defined as (visible reflectance - NIR reflectance) / (visible reflectance + NIR reflectance) or for TM (band 2 - band 5) / (band 2 + band 5). Snow and cloud discrimination is also achieved with the NDSI, though confusion with cirrus (ice clouds) is a problem. Water may also have a high NDSI and thus be confused with snow but, that confusion is largely eliminated by use of far red threshold test which discriminates water from snow because water absorbs whereas snow reflects through the red. If observation results lie in the snow decision region of the decision rule, the pixel is identified as snow covered.

TM data is converted to radiance then reflectance using methods described by [3] using pre-flight gains and offsets, or by using recorded gains and offsets [4] when available, prior to applying the snow decision tests. We have found that use of observed reflectances increases the accuracy of snow cover identification. MODIS data input will be at-sensor reflectances. Work is in progress to incorporate atmospheric correction.

In addition to the criteria tests and decision rules for snow, the full-up version of SNOMAP will contain internal checks for data integrity that will affect algorithm flow in cases of missing or out-of-range data. During execution of the algorithm, several pieces of metadata are accumulated to provide summary information with the snow cover map and serve as indicators of quality assessment (QA). Metadata such as counts of out-of-range data and total snow area are generated and written as attributes in the HDF output file. A general QA flag based on metadata and QA criteria rules is also written as an attribute.

SNOMAP at the second level composites the results of the swath outputs from overlapping orbits into a daily snow cover product. An intermediate algorithm assembles all the swaths into tiles of a grid, SNOMAP then employs a series of criterion tests to select the 'best' observation(s) of multiple observations. If there are multiple 'best' observations, the mode of the SNOMAP swath level result is used as the result for the day.

SNOMAP at the third level composites the level 2 results for a ten day period. The technique used is to sum the number of snow observations for that period to generate a snow cover summation product. That product contains the number of days that a cell was snow covered, along with summary metadata of snow cover.

RESULTS & DISCUSSION

Runs have been undertaken on over 25 TM scenes to generate snow cover maps. Snow cover extent identified by

SNOMAP has agreed to within a few percent of snow cover identified with intensive classification methods (e.g. supervised classification and spectral mixture modelling [2]) on several TM scenes. Identified snow extent has also agreed with ground observations and with regional snow maps generated by the National Operational Hydrologic Remote Sensing Center (NOHRSC). SNOMAP continues to be validated against other techniques and data sources of snow cover.

The most commonly encountered error in SNOMAP is confusion of cirrus clouds with snow. No consistent trend has been observed in confusing snow with cirrus clouds. In some situations cirrus clouds over non-snow covered land may be identified as snow, while in other seemingly similar situations it will not; cirrus clouds over snow are also inconsistently confused. Means of sorting out this confusion are being explored. Much of the confusion may be alleviated with the integration of the MODIS cloud mask, developed by another MODIS investigator team, which has the capability of identifying cirrus clouds.

Solar zenith angle (SZA) has been observed to have an effect on identification of snow. A study is in progress to determine if there is a crucial SZA above which snow identification becomes erroneous. This appears to be an issue related to high SZA. If a crucial SZA is determined, then a bound on acceptable SZAs will be incorporated into SNOMAP.

A simulated weekly snow composite has been generated with SNOMAP from a pseudo time series of TM data to demonstrate the information content of the composited product. SNOMAP higher level products have been generated with simulated MODIS data. Simulated MODIS data are used to test the flow of SNOMAP through all levels of product generation. The higher level products exhibit consistent snow cover extent results among levels. Lack of validation data for composites precludes significant comment to be made for the composited snow covers.

SUMMARY

Results obtained with SNOMAP and review of products and techniques by the community [1,2] indicate that the snow identification technique and products being developed will be of general utility to sections of the community. Research is continuing to improve snow identification techniques, including conditional bounding of factors such as SZA, defining metadata and quality indicators for the SNOMAP products. Concurrent with research is the programming task of preparing the program code to be run in the production environment of EOSDIS. Expectations are that MODIS will be launched aboard the EOS AM platform in mid 1998, and that data product generation will begin shortly after MODIS is declared operational.

REFERENCES

- [1] D.K. Hall, (Editor) "First Moderate Resolution Imaging Spectroradiometer (MODIS) Snow and Ice Workshop", NASA Conference Publication 3318, Sept 13-14, 1995, Greenbelt, MD
- [2] D.K. Hall, G.A. Riggs, and V.V. Salomonson. "Development of Methods for Mapping Global Snow Cover Using Moderate Resolution Imaging Spectroradiometer Data", Remote Sens. Environ. 54:127-140 (1995).
- [3] B.L. Markham and J.L. Barker, "Thematic Mapper Bandpass Solar Exoatmospheric Irradiances", Int. J. Remote Sens., 8:517-523 (1987).
- [4] P.S. Chavez, "Radiometric Calibration of Landsat Thematic Mapper Multispectral Images", Photogram. Eng. Remote Sens., 55:1285-1294 (1989).